

Supporting information

Self-energy correction and numerical simulation for efficiency lead-free double perovskite solar cells

The effective masses of electrons (m^*_e) and holes (m^*_h) are correlated with the curves at the top of VB and bottom of CB by using relation:

$$\frac{1}{m} = \frac{1}{\hbar^2} \frac{\delta^2 E}{\delta k^2}$$

The carrier mobility is calculated employing a simple approach based on deformation potential theory as shown below:

$$\mu = \frac{8\pi^{1/2} \hbar^4 e c_{ii}}{3(m^*)^{5/2} (k_B T)^{3/2} E_1^2}$$

\hbar is the reduced Planck constant, e is the element charge, c_{ii} is the elastic constant, m^* is the effective mass of charge, k_B is the Boltzmann constant, T is the absolute temperature, and E_1 is the deformation potential.

The optical properties have been determined from the dielectric function $\varepsilon = \varepsilon_1 + i\varepsilon_2$, where the imaginary part ε_2 can be determined from the momentum matrix elements between the unoccupied and occupied wave functions and the real part ε_1 can be obtained from the imaginary part ε_2 by using the Kramer-Kronig relation given by:

$$\varepsilon_1 = 1 + 2P/\pi \int \frac{\omega' \varepsilon_2(\omega')}{(\omega'^2 - \omega^2)} d\omega'$$

VB/CB effective density of states is caculated by following formula:

$$N = 2\left(\frac{m^*k_0T}{2\pi\hbar^2}\right)^{3/2}$$

The approximate thermal velocities of electrons and holes is caculated with

$$v_{th} = \sqrt{\frac{3KT}{m^*}}$$

material	band gap	material	band gap	material	band gap
Cs ₂ AgBiBr ₆	1.33	Cs ₂ AgCuBr ₆	0.00	Cs ₂ TlBiBr ₆	1.71
Cs ₂ AgSbBr ₆	0.88	Cs ₂ AgTiBr ₆	0.00	Cs ₂ LiBiBr ₆	2.94
Cs ₂ AgScBr ₆	2.73	Cs ₂ AgVBr ₆	0.00	Cs ₂ NaBiBr ₆	3.05
Cs ₂ AgInBr ₆	0.20	Cs ₂ AgCrBr ₆	0.76	Cs ₂ KBiBr ₆	3.42
Cs ₂ AgAlBr ₆	1.19	Cs ₂ AgMnBr ₆	0.00	Cs ₂ RbBiBr ₆	3.41
Cs ₂ AgGaBr ₆	0.00	Cs ₂ AgFeBr ₆	0.00	Cs ₂ CuBiBr ₆	0.63
Cs ₂ AgTlBr ₆	0.00	Cs ₂ AgCoBr ₆	0.23	Cs ₂ AuBiBr ₆	0.24
Cs ₂ AgCdBr ₆	0.00	Cs ₂ AgNiBr ₆	0.00		

Table S1 The band gaps of 22 kinds of lead-free double materials by PBE method.

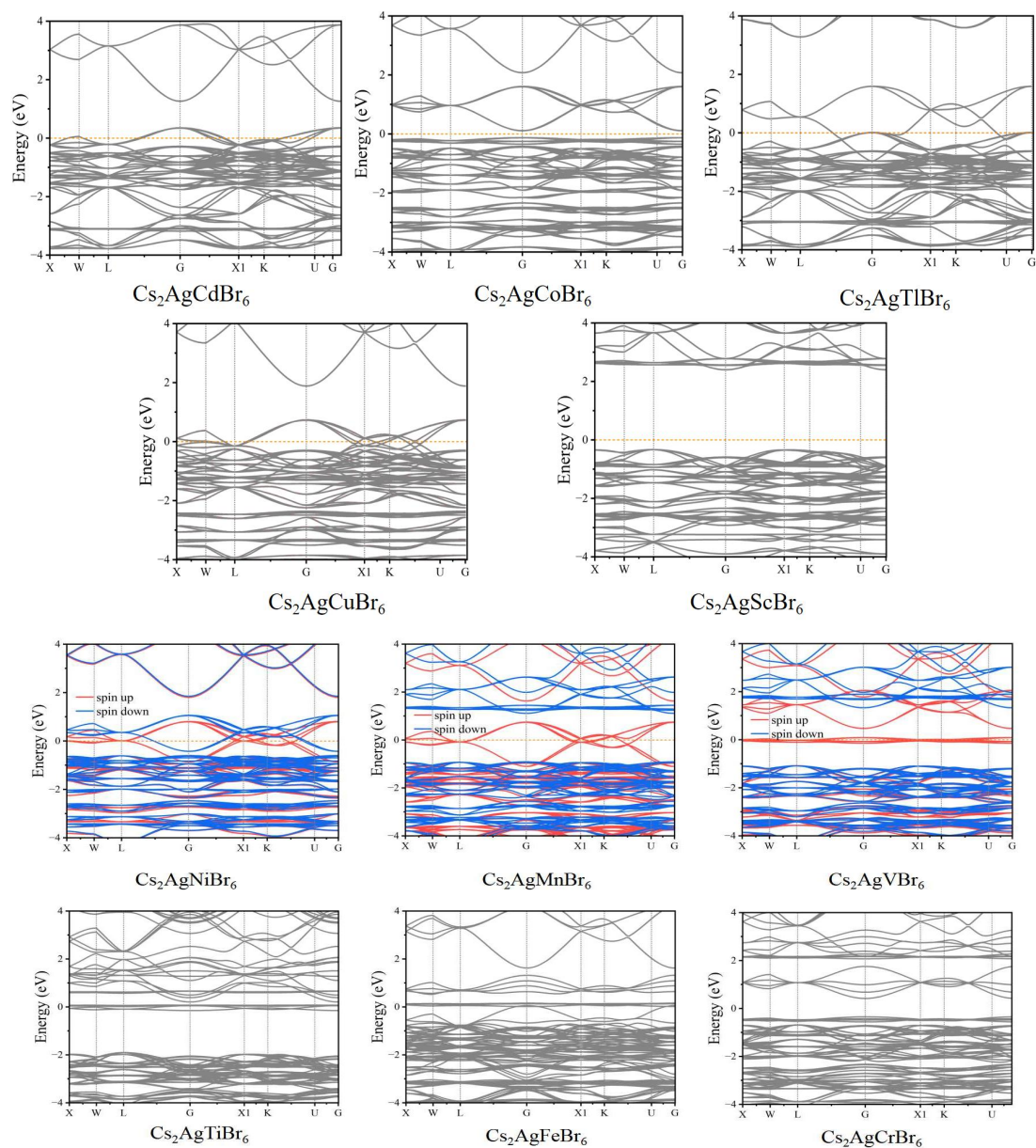


Figure S1 The band gap of $\text{Cs}_2\text{B}'\text{B}''\text{Br}_6$ with magnetic elements. (5 materials ($\text{Cs}_2\text{AgCdBr}_6$, $\text{Cs}_2\text{AgCoBr}_6$, $\text{Cs}_2\text{AgCuBr}_6$, $\text{Cs}_2\text{AgScBr}_6$, $\text{Cs}_2\text{AgTiBr}_6$) are calculated to be non-magnetic. And there are 6 materials with magnetic properties ($\text{Cs}_2\text{AgMnBr}_6$, $\text{Cs}_2\text{AgNiBr}_6$, $\text{Cs}_2\text{AgVBr}_6$, $\text{Cs}_2\text{AgTiBr}_6$, $\text{Cs}_2\text{AgCrBr}_6$, $\text{Cs}_2\text{AgFeBr}_6$.)

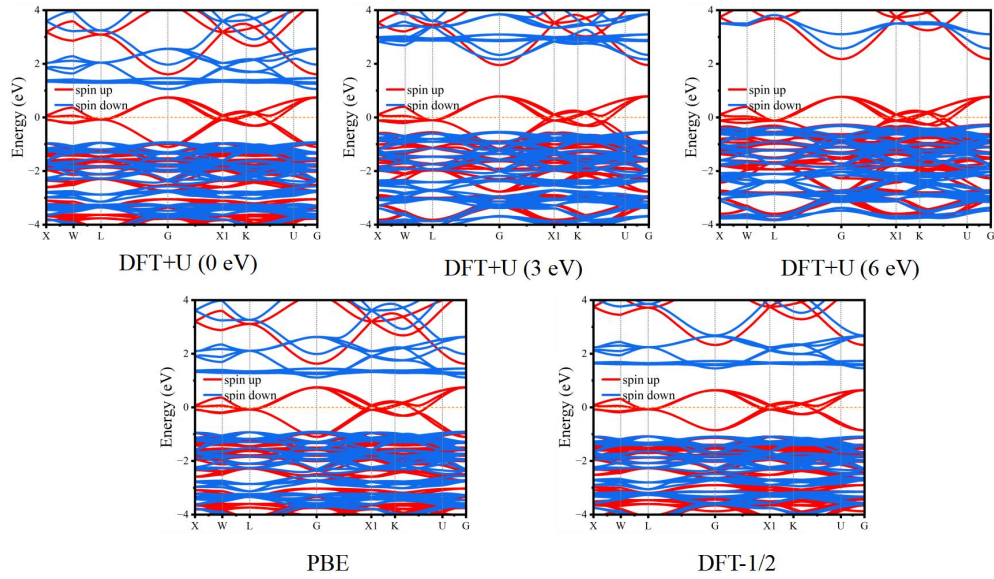


Figure S2. The band gap of $\text{Cs}_2\text{AgMnBr}_6$ with PBE, DFT-1/2 and DFT+U ($U_{\text{eff}} = 0, 3, 6$ eV) method.

Table S2 The ground state and ferromagnetic or antiferromagnetic energy of magnetic materials. (The antiferromagnetic energies of $\text{Cs}_2\text{AgTiBr}_6$, $\text{Cs}_2\text{AgCrBr}_6$ and $\text{Cs}_2\text{AgFeBr}_6$ are lower than the ferromagnetic energies, showing the antiferromagnetic ground states, while $\text{Cs}_2\text{AgMnBr}_6$, $\text{Cs}_2\text{AgNiBr}_6$ and $\text{Cs}_2\text{AgVBr}_6$ show the ferromagnetic ground states.)

material	$\text{Cs}_2\text{AgMnBr}_6$	$\text{Cs}_2\text{AgNiBr}_6$	$\text{Cs}_2\text{AgVBr}_6$	$\text{Cs}_2\text{AgTiBr}_6$	$\text{Cs}_2\text{AgCrBr}_6$	$\text{Cs}_2\text{AgFeBr}_6$
ferromagnetic energy (eV)	-136.67	-116.12	-139.11	-140.06	-139.77	-129.81
antiferromagnetic energy (eV)	-136.33	-116.04	-139.02	-140.07	-139.81	-130.15
ground state	FM	FM	FM	AFM	AFM	AFM

Table S3 The band gap and magnetic moment of 11 materials with magnetic elements.

material	E _g (eV)	M (μ _B)	material	E _g (eV)	M (μ _B)
Cs ₂ AgCdBr ₆	0.00	0.00	Cs ₂ AgMnBr ₆	0.00	14.84
Cs ₂ AgCoBr ₆	0.23	0.00	Cs ₂ AgNiBr ₆	0.00	1.86
Cs ₂ AgCuBr ₆	0.00	0.00	Cs ₂ AgVBr ₆	0.00	7.17
Cs ₂ AgScBr ₆	2.73	0.00	Cs ₂ AgTiBr ₆	0.00	0.00
Cs ₂ AgTlBr ₆	0.00	0.00	Cs ₂ AgCrBr ₆	0.76	0.00
			Cs ₂ AgFeBr ₆	0.00	0.00

Table S4 The decomposition enthalpy and binding energy of Cs₂B'B''Br₆ (B' = Ag, Au, Cu; B'' = Bi, Al, Sb, In).

material	binding energy (eV)	decomposition enthalpy ΔH _d
Cs ₂ AgBiBr ₆	-2.92	-0.057
Cs ₂ CuBiBr ₆	-2.97	-0.081
Cs ₂ AuBiBr ₆	-2.87	-0.061
Cs ₂ AgSbBr ₆	-2.88	-0.064
Cs ₂ AgInBr ₆	-2.81	-0.050
Cs ₂ AgAlBr ₆	-3.00	-0.180

The binding energy is calculated by

$$\Delta E_{(Cs_2B'B''Br_6)} = \frac{E_{tot}(Cs_2B'B''Br_6) - k \times E_s(Cs) - l \times E_s(B') - m \times E_s(B'') - n \times E_s(Br)}{k+l+m+n}$$

The decomposition enthalpy (ΔH_d) is calculated by

$$\Delta H_d = E_{rxn} = E_{ABCD} - E_{A-B-C-D}$$

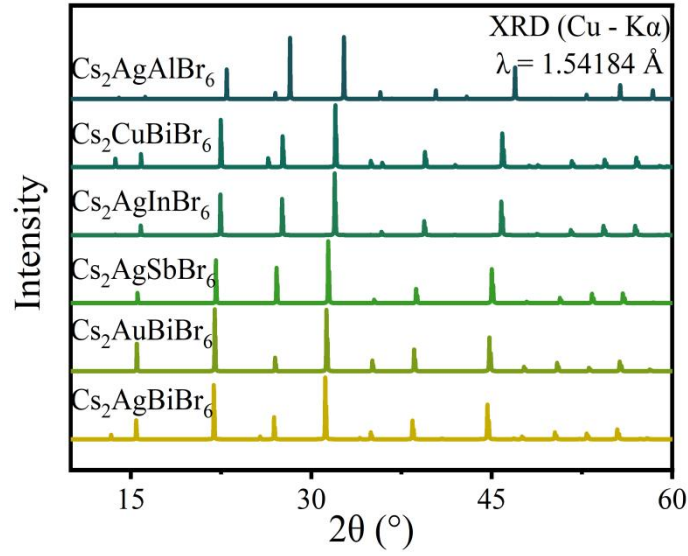


Figure S3 XRD patterns of all selected materials have been shown. It clearly shows that they all have similar diffraction peaks, indicating their similar crystal structures.

Table S5 The calculated elastic constants C_{11} , C_{12} , C_{44} , Bulk modulus B , Shear modulus G , Young modulus E , Pugh's ratio (B/G), Poisson's ratio (ν) of $\text{Cs}_2\text{B}'\text{B}''\text{Br}_6$ ($\text{B}' = \text{Ag, Au, Cu}$; $\text{B}'' = \text{Bi, Al, Sb, In}$).

material	C_{11}	C_{12}	C_{44}	$C_{12}-C_{44}$	B	G	E	B/G	ν
$\text{Cs}_2\text{AgBiBr}_6$	34.52	10.26	9.96	0.3	18.35	10.78	27.04	1.70	0.25
$\text{Cs}_2\text{AgSbBr}_6$	25.83	10.55	9.91	0.64	15.64	8.93	22.51	1.75	0.26
$\text{Cs}_2\text{AuBiBr}_6$	16.85	13.67	6.28	7.39	14.73	3.64	10.09	4.04	0.39
$\text{Cs}_2\text{CuBiBr}_6$	17.31	12.68	8.88	3.8	14.22	5.21	13.92	2.73	0.33
$\text{Cs}_2\text{AgAlBr}_6$	14.29	12.47	11.23	1.24	13.08	4.56	12.25	2.87	0.34
$\text{Cs}_2\text{AgInBr}_6$	13.17	13.03	8.71	4.32	13.07	2.51	7.07	5.21	0.41

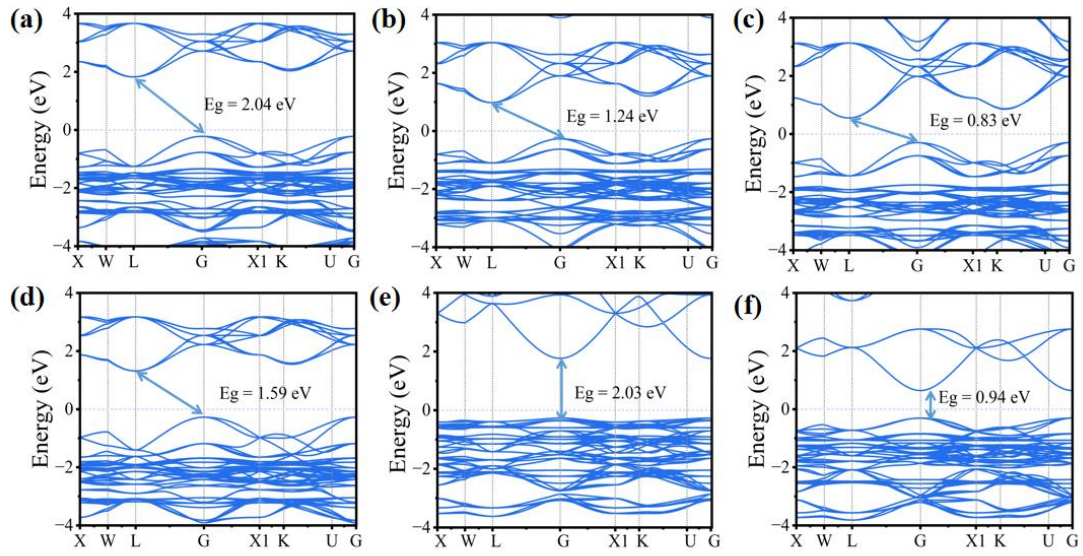


Figure S4 Band gap for six materials (a) $\text{Cs}_2\text{AgBiBr}_6$ (b) $\text{Cs}_2\text{CuBiBr}_6$ (c) $\text{Cs}_2\text{AuBiBr}_6$ (d) $\text{Cs}_2\text{AgSbBr}_6$ (e) $\text{Cs}_2\text{AgAlBr}_6$ and (f) $\text{Cs}_2\text{AgInBr}_6$.

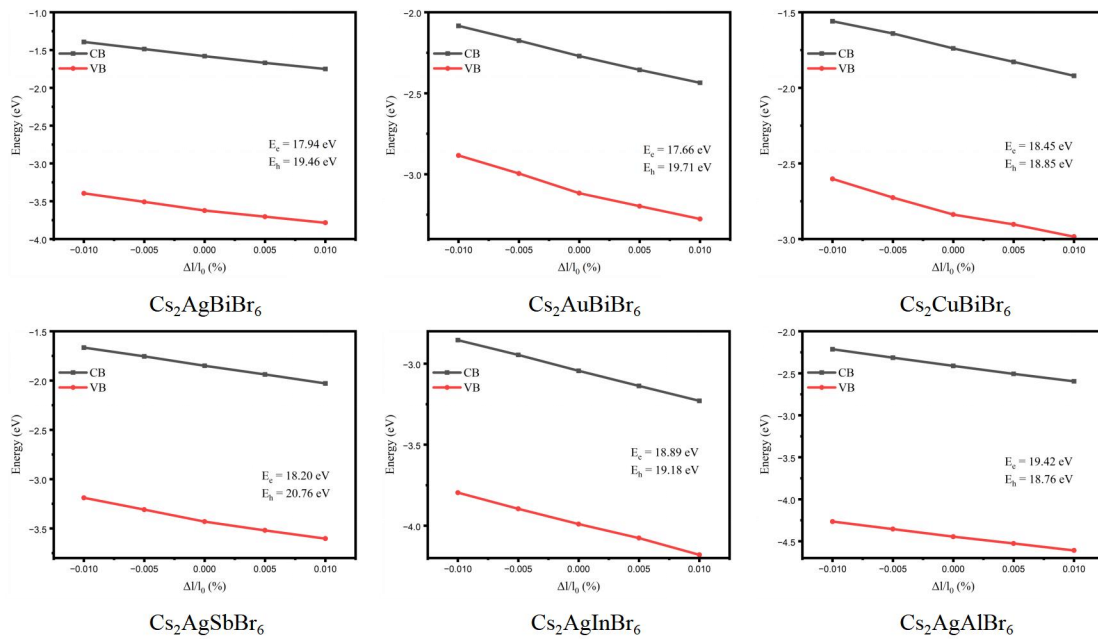


Figure S5. The deformation potential of $\text{Cs}_2\text{B}'\text{B}''\text{Br}_6$ ($\text{B}' = \text{Ag, Au, Cu}$; $\text{B}'' = \text{Bi, Al, Sb, In}$).

The shift in the band energy (ΔE) with respect to a small lattice dilation (Δl) along a lattice (l_0) direction ($E_1 = \Delta E / [\Delta l / l_0]$) is interpreted as the deformation potential.

We have calculated the band structure of unit cells at five selected deformed lattice constants: $0.990a_0$, $0.995a_0$, $1.000a_0$, $1.005a_0$ and $1.010a_0$, where a_0 is lattice parameter without any strain.

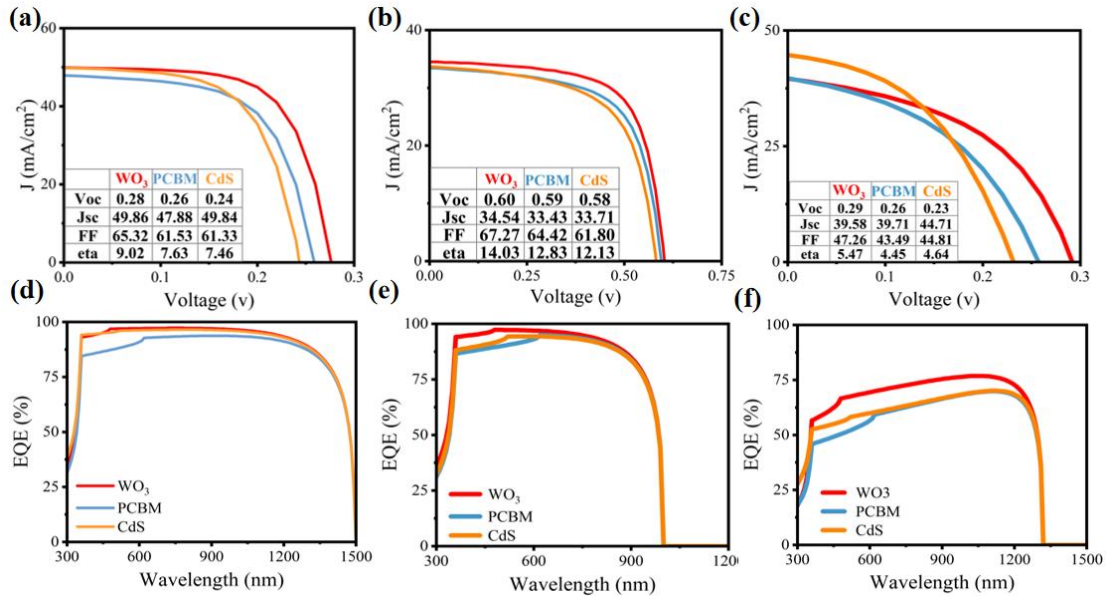


Figure S6 J-V characteristic and EQE-wavelength of PSC under initial simulation condition, respectively (a,d) for $\text{Cs}_2\text{AuBiBr}_6$, (b,e) for $\text{Cs}_2\text{CuBiBr}_6$, (c,f) for $\text{Cs}_2\text{AgInBr}_6$.

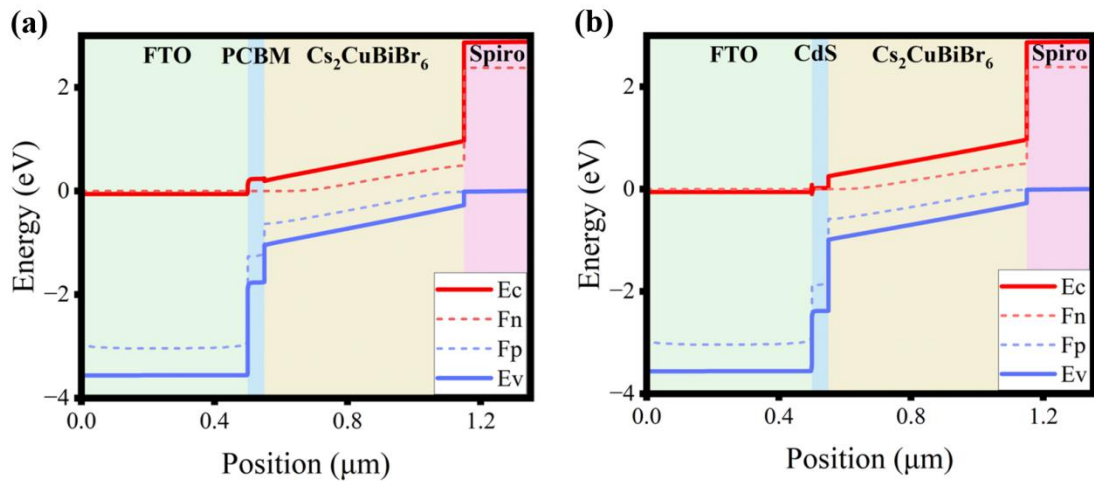


Figure S7 The electronic band diagram of the proposed photovoltaic solar cell with (a) FTO/PCBM/ $\text{Cs}_2\text{CuBiBr}_6$ /Spiro-OMeTAD/Ag configuration and (b) FTO/CdS/ $\text{Cs}_2\text{CuBiBr}_6$ /Spiro-OMeTAD/Ag configuration.